Shear-Induced Orientation of a Rigid Surfactant Mesophase

Mohit Singh,† Vivek Agarwal,‡ Daniel De Kee,† Gary McPherson,§ Vijay John,*,† and Arijit Bose*,‡

Department of Chemical Engineering, Tulane University, New Orleans, Louisiana 70118, Department of Chemical Engineering, University of Rhode Island, Kingston, Rhode Island 02881, and Department of Chemistry, Tulane University, New Orleans, Louisiana 70118

Received February 3, 2004

An optically clear, crystalline, gel-like mesophase is formed by the addition of water to a micellar solution consisting of a mixture of 0.85 M anionic surfactant sodium bis(2-ethylhexyl) sulfosuccinate (AOT) and a 0.42 M zwitterionic surfactant phosphatidylcholine (lecithin) in isooctane. At 25 °C and water to AOT molar ratio of 70, the system has a columnar hexagonal microstructure with randomly oriented domains. The shear-induced orientation and subsequent relaxation of this structure were investigated by rheological characterization and small-angle neutron scattering (SANS). The rheological response implies that the domains align under shear, and remain aligned for several hours after cessation of shear. Shear-SANS confirms this picture. The sheared gel mesophase retains its alignment as the temperature is increased to 57 °C, indicating the potential to conduct templated polymer and polymer−ceramic composite materials synthesis in aligned systems.

Introduction

Over the past decade there has been significant interest in the effect of magnetic,[1] electrical,[2] and shear[3] fields on structural changes induced in lyotropic systems. The response of lyotropic phases under a directing flow field is of special interest, as it leads to useful insights into the relationship between the macroscopic flow and micro-/mesoscopic structures in the flow media.[4,5] A variety of responses involving phase transitions from isotropic to ordered,[6] ordered to isotropic,[7] ordered to ordered,[8] and shear alignment of polycrystalline mesophases[9] have been observed. A wide range of lyotropic systems exhibit shear alignment, including block copolymers,[10] wormlike micelles,[11,12] and surfactant lamellar, cubic, and hexagonal phases.[13,14,15] Rheology along with experimental techniques such as flow birefringence,[16,17] NMR,[18,19] optical and electron microscopy,[20,21] X-ray scattering,[15,22] small-angle light scattering (SALS)[23] and, in recent years, small-angle neutron scattering (SANS),[24] have been used to observe and elucidate the shear alignment of mesophases.

The rheology of soft colloids has been studied extensively in order to understand the correlation between the rheological response and microstructure.[25] Structured soft colloids are especially interesting as they may be used as templates for materials synthesis. Among structured soft colloids, the shear response of lamellar phases has been studied extensively.[26−29] Shear flow, in some cases, leads to alignment and/or a rate-dependent reorientation of the lamellae.[30] A number of research groups have observed onion phases or multilayer vesicles (MLVs) upon shearing

* To whom correspondence may be addressed: Vijay John, 504 865-5883, vijay.john@tulane.edu.; Arijit Bose, 401 874-2804, bosea@egr.uri.edu.

† Department of Chemical Engineering, Tulane University.

‡ Department of Chemical Engineering, University of Rhode Island.

§ Department of Chemistry, Tulane University.

(1) Fischer, A.; Hoffmann, H.; Medick, P.; Roessler, E. *J. Phys. Chem. B* **2002**, *106* (26), 6821.
(2) Huang, L.; Wang, H.; Wang, Z.; Mitra, A.; Zhao, D.; Yan, Y. *Chem. Mater.* **2002**, *14* (2), 876.
(3) Richtering, W. *Curr. Opin. Colloid Interface Sci.* **2001**, *6*(5,6), 446.
(4) Burghardt, W. R. *Macromol. Chem. Phys.* **1998**, *199* (4), 471.
(5) Kim, W. J.; Yang, S. M. *Adv. Mater.* (*Weinheim, Germany*) **2001**, *13* (15), 1191.
(6) Wunderlich, I.; Hoffmann, H.; Rehage, H. *Rheol. Acta* **1987**, *26* (6), 532.
(7) Volkova, O.; Cutillas, S.; Bossis, G. *Phys. Rev. Lett.* **1999**, *82* (1), 233.
(8) Krishnamoorti, R.; Silva, A. S.; Modi, M. A.; Hammouda, B. *Macromolecules* **2000**, *33* (10), 3803.
(9) Schmidt, G.; Richtering, W.; Lindner, P.; Alexandridis, P. *Macromolecules* **1998**, *31* (7), 2293.
(10) Hamley, I. W. *J. Phys.: Condens. Matter* **2001**, *13* (33), R643.
(11) Angelico, R.; Olsson, U.; Mortensen, K.; Ambrosone, L.; Palazzo, G.; Ceglie, A. *J. Phys. Chem. B* **2002**, *106* (10), 2426.
(12) Shchipunov, Y. A.; Hoffmann, H. *Rheol. Acta* **2000**, *39* (6), 542.
(13) Berghausen, J.; Zipfel, J.; Diat, O.; Narayanan, T.; Richtering, W. *Phys. Chem. Chem. Phys.* **2000**, *2* (16), 3623.
(14) Linemann, R.; Laeuger, J.; Schmidt, G.; Kratzat, K.; Richtering, W. *Rheol. Acta* **1995**, *34* (5), 440.
(15) Ramos, L.; Molino, F.; Porte, G. *Langmuir* **2000**, *16* (14), 5846.
(16) Honladarom, K.; Burghardt, W. R.; Baek, S. G.; Cementwala, S.; Magda, J. J. *Macromolecules* **1993**, *26*, 772.
(17) Schmidt, G.; Nakatani, A. I.; Han, C. C. *Rheol. Acta* **2002**, *41* (1−2), 45.
(18) Grabowski, D. A.; Schmidt, C. *Macromolecules* **1994**, *27*, 2632.
(19) Kilfoil, M. L.; Callaghan, P. T. *Macromolecules* **2000**, *33* (18), 6828.
(20) Schmidt, G.; Muller, S.; Schmidt, C.; Richtering, W. *Rheol. Acta* **1999**, *38* (6), 486.
(21) Chen, Z.-R.; Issaian, A.; Kornfield, J. A.; Smith, S. D.; Grothaus, J. T.; Satkowski, M. M. *Macromolecules* **1997**, *30* (23), 7096.
(22) Pople, J. A.; Hamly, I. W.; Daikun, G. P. *Rev. Sci. Instrum.* **1998**, *69*, 3015.
(23) Zipfel, J.; Berghausen, J.; Lindner, P.; Richtering, W. *J. Phys. Chem. B* **1999**, *103*(15), 2841.
(24) Jindal, V. K.; Kalus, J.; Pilsl, H.; Hoffmann, H.; Lindner, P. *J. Phys. Chem.* **1990**, *94* (7), 3129.
(25) Larson, R. G. *The Structure and Rheology of Complex Fluids*; Oxford University Press: Oxford, 1999.
(26) Bergenholtz, J.; Wagner, N. J. *Langmuir* **1996**, *12* (13), 3122.
(27) Diat, Olivier; Roux, Didier; Nallet, Frederic *J. Phys. II* **1993**, *3* (9), 1427.
(28) Panizza, P.; Roux, D.; Vuillaume, V.; Lu, C.-Y. D.; Cates, M. E. *Langmuir 1996, 12* (2), 248.
(29) Nettesheim, F.; Zipfel, J.; Olsson, U.; Renth, F.; Lindner, P.; Richtering, W. *Langmuir* **2003**, *19* (9), 3603.
(30) Berghausen, J.; Zipfel, J.; Lindner, P.; Richtering, W. *Europhys. Lett.* **1998**, *43* (6), 683.

10.1021/la049700y CCC: $27.50
Published on Web 06/08/2004

a lamellar phase.[26,31,32,33] Detailed studies have been conducted in order to understand the mechanism of this shear-induced transition[29] and to elucidate the microstructure of the MLVs formed.[34]

The shear response of hexagonal systems is of particular interest and the focus of this work. In earlier work on other systems, Morrison and co-workers[35] have demonstrated that the cylindrical domains in polystyrene−polybutadiene−polystyrene triblock copolymer orient in the flow direction with little change in the domain size or shape. Hamilton and co-workers[36] showed that a dilute surfactant solution of highly extended charged threadlike micelles, consisting of cetyltrimethylammonium 3,5-dichlorobenzoate and cetyltriammonium bromide align along the flow direction. With a detailed analysis of the SANS data, the authors reached the unambiguous conclusion that these micelles shear align into the hexagonal phase. Since these early reports, several other researchers have also reported shear-aligned hexagonal phases. Anisotropic structures with hexagonal order from shear alignment of rods/cylinders[37,38] and copolymer hexagonal phases[39,40] in flow direction have been reported. Shear response of lyotropic hexagonal phases, consisting of aqueous solutions of block copolymers[9] and nonionic surfactants,[41,42] has been studied, and alignment in direction of flow has been reported in most of these cases. Richtering and co-workers have demonstrated shear orientation of aqueous mixtures of a nonionic surfactant perpendicular to the flow direction for low shear rates due to high elasticity of the hexagonal liquid crystalline phase.[43] Polycrystalline systems, such as aqueous triblock copolymer solutions of similar block structures,[44] have also been investigated. The authors correlate the flow curve and the SAXS patterns to illustrate shear banding in the case of block copolymer polycrystalline mesophases.[44] Rate-dependent shear melting, evident from the SAXS patterns, is observed in lyotropic hexagonal phases consisting of a quaternary mixture of sodium dodecyl sulfate, pentanol, cyclohexane, and brine that can be correlated with the critical rates in the flow curve.[15] Recently Ahir and co-workers have reported a strain-dependent two-dimensional melting of the hexagonal order in a surfactant solution of Triton X100 in water.[45]

In this paper, we examine shear alignment of hexagonally arranged cylinders consisting of an anionic surfactant, AOT (sodium bis(2-ethylhexyl) sulfosuccinate), and a zwitterionic surfactant, lecithin (α-phosphatidylcholine), swollen with water, and dispersed in an organic phase. We have recently described this surfactant-based rigid gel-like mesophase containing 0.85 M AOT, 0.42 M lecithin, isooctane, and water.[46,47] A 0.85 M AOT solution in isooctane contains spherical inverse micelles. At 25 °C, this solution can incorporate water to a water/AOT molar ratio of approximately 45 prior to phase separation. The zwitterionic surfactant, lecithin, forms long entangled wormlike micelles in isooctane at 0.42 M. At 25 °C, these micelles can incorporate water to a water/lecithin molar ratio of about 20 at room temperature.[48] The combination of AOT and lecithin with differing packing parameters and spontaneous curvatures, leads to a highly rigid gel-like surfactant mesophase that can incorporate significantly higher water contents. As an example, when AOT and lecithin are simultaneously dissolved in isooctane at concentrations of 0.85 and 0.42 M, respectively, the solution follows Newtonian behavior with a viscosity of 0.1 Pa·s at 25 °C. When water is added to the system, the viscosity increases and the solution becomes a rigid gel phase when the water content reaches $W_0 = 70$ (W_0 is the molar ratio of water to AOT). The surfactant mesophase remains rigid and single phase for W_0 of 70−200, and typical low shear viscosities over this W_0 range are on the order of 10^6 Pa·s.

Our earlier work on SANS characterization of this system has shown that at 25 °C and $W_0 = 70$, the mesophase has the reverse hexagonal columnar structure (H_{II}).[46] As the water content is increased, the mesophase goes through a coexistence region ($\sim W_0 = 120$) containing both columnar hexagonal and lamellar (L_α) phases and eventually forms a predominantly lamellar phase at water content of 170 and above. The transition from hexagonal to lamellar also occurs as the temperature is increased from 25 to 65 °C, with the lower temperatures favoring the hexagonal phase.

Our present study focuses on the H_{II} phase at $W_0 = 70$ at ambient temperature and examines the role of shear in aligning the hexagonal cylinders through both rheological and SANS characterizations. A pioneering study of the shear alignment of the swollen H_I hexagonal phase was recently reported by Ramos and co-workers.[15] These authors started with a quaternary mixture of sodium dodecyl sulfate, pentanol, cyclohexane, and brine that yields, at rest, a structure consisting of oil cylinders of radius 15 nm, immersed in water and arranged in a two-dimensional (2D) hexagonal lattice with a lattice parameter of 33 nm. The authors report a shear thinning system with a typical low shear viscosity of ∼3 Pa·s, and a yield stress value of 8.8 Pa.[15] In the present study we focus on a highly rigid and viscous H_{II} phase with low shear viscosity of the order of 10^5 Pa·s and a yield stress value of ∼55 Pa. The present study complements the observations reported in the literature in two ways: we demonstrate a flow-induced alignment in a very rigid polycrystalline surfactant mesophase that does not involve shear melting, and for the first time we report retention of alignment upon heating a shear-aligned mesophase.

(31) Soubiran, L.; Staples, E.; Tucker, I.; Penfold, J.; Creeth, A. *Langmuir* **2001**, *17* (26), 7988.
(32) Muller, S., Borschig, C., Gronski, W., Schmidt, C., Roux, D. *Langmuir* **1999**, *15*, 7558.
(33) Le, T. D.; Olsson, U.; Mortensen, K.; Zipfel, J.; Richtering, W. *Langmuir* **2001**, *17* (4), 999.
(34) Gulik-Krzywicki, T.; Dedieu, J. C.; Roux, D.; Degert, C.; Laversanne, R. *Langmuir* **1996**, *12* (20), 4668.
(35) Morrison, F. A.; Winter, H. H. *Macromolecules* **1989**, *22*, 3533.
(36) Hamilton, W. A.; Butler, P. D.; Baker, S. M.; Smith, G. S.; Hayter, John B.; Magid, L. J.; Pynn, R. *Phys. Rev. Lett.* **1994**, *72* (14), 2219.
(37) Scott, Diane B.; Waddon, Alan J.; Lin, Ye Gang; Karasz, Frank E.; Winter, H. Henning. *Macromolecules* **1992**, *25* (16), 4175.
(38) Hamilton W. A.; Butler P. D.; Magid L. J.; Han Z.; Slawecki T. M. *Phys. Rev. E* **1999**, *60* (2 Pt A), R1146.
(39) Tepe, T.; Schulz, M. F.; Zhao, J.; Tirrell, M.; Bates, F. S.; Mortensen, K.; Almdal, K. *Macromolecules* **1995**, *28* (8), 3008.
(40) Daniel, C.; Hamley, I. W.; Mingvanish, W.; Booth, C. *Macromolecules* **2000**, *33*, 2163.
(41) Schmidt, G.; Mueller, S.; Lindner, P.; Schmidt, C.; Richtering, W. *J. Phys. Chem. B* **1998**, *102*(3), 507.
(42) Terry, A. E.; Odell, J. A.; Nicol, R. J.; Tiddy, G. J. T.; Wilson, J. E. *J. Phys. Chem. B* **1999**, *103* (50), 11218.
(43) Richtering, W.; Lauger, J.; Linemann, R. *Langmuir* **1994**, *10*, 4374.
(44) Eiser, E.; Molino, F.;, Porte, G.; Pithon, X. *Rheol. Acta* **2000**, *39*, 201.
(45) Ahir, S. V.; Petrov, P. G.; Terentjev, E. M. *Langmuir* **2002**, *18* (24), 9140
(46) Simmons, B. A.; Irvin, G. C.; Agarwal, V.; Bose, A.; John, V. T.; McPherson, G. L.; Balsara, N. P. *Langmuir* **2002**, *18* (3), 624.
(47) Li, S.; Irvin, G. C.; Simmons, B.; Rachakonda, S.; Ramannair, P.; Banerjee, S.; John, V. T.; McPherson, G. L.; Zhou, W.; Bose, A. *Colloids Surf., A* **2000**, *174*, 275.
(48) Scartazzini, R.; Luisi, P. L. *J. Phys. Chem.* **1988**, *92*, 829. Capitani, D.; Segre, A. L.; Sparapani, R.; Giustini, M.; Scartazzini, R.; Luisi, P. L. *Langmuir* **1991**, *7*, 250. Schurtenbergere, P.; Scartazzini, R.; Luisi, P. L. *Rheol. Acta* **1989**, *28*, 372. Luisi, P. L.; Scartazzini, R.; Haering, G.; Schurtenberger, P. *Colloid Polym. Sci.* **1990**, *268*, 356.

Crystalline mesophases are of significant interest in the templated synthesis of nanostructured materials, because the spatial immobilization of the hydrophobic and the hydrophilic regions may allow the formation of extended structures that are organized over multiple length scales.[49] The prospect of forming functional materials in the surfactant mesophase under an aligning shear may lead to new opportunities in materials synthesis. In this paper we examine the rheological characteristics of the $W_0 = 70$ mesophase and complement these studies with SANS measurements. The objectives of this work are to understand whether the domains of the columnar hexagonal structure can be aligned through shear, the characteristics of the shear alignment, and the relaxation characteristics of the system after the cessation of shear.

Experimental Section

Chemicals. Phosphatidylcholine (95% pure, lecithin-extracted from soybeans) was obtained from Avanti Polar Lipids, Inc. Sodium bis(2-ethylhexyl) sulfosuccinate (AOT) and 2,2,4-trimethylpentane (isooctane, 99% purity) were purchased from Sigma. Deuterium oxide (99.9%) was purchased from Cambridge Isotopes Laboratory. Either D_2O or a mixture of D_2O and distilled water was used for making the samples. All chemicals were used without further treatment and/or purification.

Sample Preparation. AOT (0.85 M) and lecithin (0.42 M) were dissolved in isooctane by sonicating in a water bath at 38 °C until a clear yellow solution was obtained. D_2O or a mixture of D_2O and distilled water was added incrementally until a value $W_0 = 70$ was reached. After each addition of D_2O, the sample was sonicated in a warm water bath at 50 °C and vortex mixed until a clear solution/gel was obtained. The sample was then removed from the water bath, centrifuged at 1000 RCF to remove air bubbles, and allowed to cool to ambient conditions. At $W_0 = 70$ the surfactant system is slightly above the gelation threshold and is much more rigid if distilled water is used instead of D_2O.

Rheological tests were conducted on a TA instruments AR-2000 constant stress (controlled strain and controlled rate is achieved through an extremely sensitive feed back loop) rheometer with a built-in temperature and gap calibration. The cone and plate geometry, with a cone angle of 1° and diameter 40 mm, was used. The cone and plate geometry applies a uniform shear field through the sample and allows accurate measurement of normal stress and the storage and loss moduli G' and G'', respectively. A vendor-supplied solvent trap was used to mitigate solvent loss from the system. The cone and plate assembly was checked for slip by verifying the data with a vendor-supplied crosshatched parallel plate geometry (using the Weissenberg−Rabinowitsch correction[50] in the TA analysis software). Only the stress range in which the two geometries produced similar results was used. The rheological response showed a great dependence on the history of the sample and preshear involved in sample loading. While the trend or characteristics of a rheological response (for example, viscosity versus shear rate) was the same in all runs, the actual values of measured variable such as viscosity showed a large standard deviation (∼30−50%) in separate loadings of the sample. The results presented here represent data obtained from a typical run. D_2O was used to make the surfactant gels for all rheological tests (except yield stress experiments where distilled water was used because of large sample volume requirements) for direct comparison with results from SANS.

In steady stress measurements, the applied stress was varied from 0.4 to 200 Pa. This upper limit of the shear stress was dictated by flow instability caused by severe edge deformation observed in the sample at higher shear rates.[51] Small amplitude oscillatory tests were also conducted in the angular frequency range of 0.05−500 rad/s at 0.5% constant strain. Hysteresis experiments were performed by ramping the shear rate linearly from 0 to 5 s^{-1} in 60 s and bringing the shear rate back to 0 in the next 60 s. Three consecutive cycles were employed. All isothermal tests were performed at 25 °C. Dynamic temperature ramp tests were performed in the temperature range 25−65 °C.

Yield stress measurements were performed at 25 °C, using a novel slotted plate device.[52] The results were further verified and confirmed by creep tests. The slotted-plate device involves a balance and a linear-motion platform to measure static yield stresses directly.

SANS measurements were carried out at the National Institute of Standards and Technology (NIST) in Gaithersburg, MD, on the 30 m NG3 beamline at the NIST Center for Neutron Research (NCNR). The SANS intensity, I_q, was recorded on a 2D detector as a function of the magnitude of the scattering vector $q = 4\pi \sin(\theta/2)/\lambda$, where θ is the scattering angle and λ is the neutron wavelength. The neutron wavelength (λ) used for this study was 6 Å with a wavelength spread of 0.147. Circular pinhole collimation was used. A 64 × 64 cm^2 detector was used with a resolution of 1 cm^2. The detector angle was set at 0°, and the sample-to-detector distance was set to 4.5 m. The beam diameter was set at 1.27 cm. The range of the scattering vector for these settings q was 0.0057−0.1039 $Å^{-1}$.

The NIST Couette shear cell, consisting of an inner quartz cylindrical stator (60 mm o.d., 0.5 mm gap) and an outer quartz cylindrical rotor (61 mm i.d.), was used. Approximately 11 mL of bubble-free sample was loaded in the outer cup, and the inner stator was lowered. This method invariably introduces some preshear to the sample, though the stator was lowered slowly to avoid this effect as best as possible. The shear rates were varied from 0 to 116.7 s^{-1}. The samples were allowed to equilibrate at each temperature for 15 min before the SANS data were acquired. After the run at 57 °C was completed, the temperature was lowered back to 25 °C. The samples were then allowed to cool for 2 h at 25 °C to ensure that thermal equilibrium was attained, following which another set of SANS measurements were made to determine if the alignment is retained after changing the temperature. The SANS data were corrected for empty cell scattering, detector sensitivity, background, the transmission of each sample and were then placed on an absolute scale.

Results and Discussion

Rheological Characterization. Let us consider the AOT + lecithin system with the two surfactants dissolved in isooctane at concentrations of 0.8 and 0.4 M, respectively. This system is a liquid that behaves as a Newtonian fluid with a viscosity in the range 0.1−1 Pa·s. As we add water to the system, at low water contents ($W_0 = 0-10$), the system continues to behave as a Newtonian liquid. With higher water contents, the viscosity increases and a gel-like phase begins to appear at a W_0 of about 70. This gel phase does not flow upon tilting the vial and is optically clear.[46] Figure 1 illustrates the non-Newtonian, shear-thinning response of this system, indicating the presence of a complex microstructure that aligns and/or breaks down at high shear rates. The presence of a stress plateau even at low shear rates indicates an early shift in the flow mechanism of the gel system, and the phenomenon has been associated with shear melting by Ramos and coworkers in a specific H_I system consisting of a quarternary mixture of sodium dodecyl sulfate, pentanol, cyclohexane, and brine.[44,15] We will explain later in this section that the phenomenon observed in our system may not be shear melting, but the alignment of polycrystalline domains along with an escalation of defects at the domain/grain boundaries that anneal quickly as the flow is stopped. The gel phase has very high viscosities at low shear rates, and a measurable yield stress of ∼55 Pa. The presence of a measurable yield stress, facilitated by direct measure-

(49) John, V.; Simmons, B.; McPherson, G.; Bose, A. *Curr. Opin. Colloid Interface Sci.* **2002**, *7* (5,6), 288.

(50) Carreau, P. J.; De Kee, D. C.; Chhabra, R. P. *Rheology of Polymeric Systems*: *Principles and Applications*; Hansen/Gardner Publications: Cincinnati, OH, 1997.

(51) Morrison, F. A. *Understanding rheology*; Oxford University Press: Oxford, 2001.

(52) Zhu, L.; Sun, N.; Papadopouluos, K.; De Kee, D. *J. Rheol.* **2001**, *45* (5). De Kee, D.; Chhabra, R. P. *Rheol. Acta* **1994**, *33*, 238.

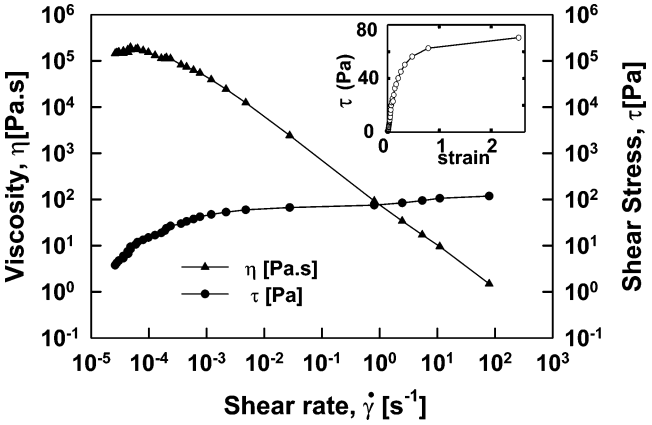

Figure 1. Viscosity (η), shear stress (τ) vs shear rate ($\dot{\gamma}$) at 25 °C for a stress-controlled steady flow experiment. The inset shows the yielding behavior through shear stress vs strain data at very low shear rates.

ment using a slotted plate device,[52] confirms a very high rigidity in the system. The inset to Figure 1 shows the steady flow data for very low shear rates, plotted as shear stress versus shear strain. The yielding behavior of the gel is readily apparent.

We performed small amplitude oscillatory tests to understand the elastic response and rigidity of the gel system. Figure 2 indicates that the gel system has high storage (G') and loss moduli (G''), and displays a predominantly solidlike behavior ($G''/G' < 1$) over a wide range of temperature and shear frequencies. This system is more elastic and rigid than typical surfactant microemulsion systems at moderate surfactant concentrations.[12,48] Figure 2a reveals that the system has a characteristic yield stress, as the elastic moduli do not cross over in the frequency range scanned.[53] An additional possibility for the frequency-independent moduli is relaxation involving multiple time scales, which we discuss after the description of the SANS results. The temperature variation of the storage and loss moduli is illustrated in Figure 2b, indicating the continued rigidity of the system over the temperature range 25−60 °C. Figure 2b also points to the interesting observation that the dynamic moduli go through a maximum as the temperature of the system is increased. Such nonmonotonic behavior of the dynamic moduli has been reported in the literature.[54−56] One plausible explanation of this response can be derived from the work of Ramos and co-workers who attribute the increase in the elastic moduli to the disorder (isotropic)−order transition and the decrease to breakage and end capping of cylindrical micelles at higher temperatures.[55] Thus, the initial increase in temperature causes stronger intercylinder interactions while scission kinetics (end capping) is enhanced at higher temperatures. The competition between the two phenomena leads to the maxima in the dynamic moduli. We note that the retention of rigidity at higher temperatures is especially useful if the mesophase is exploited for materials synthesis requiring elevated temperatures to accelerate reaction rates.

The shear rates were then cycled to understand the hysteretic response of the gel. In a typical experiment, illustrated in Figure 3, the shear stress was monitored as

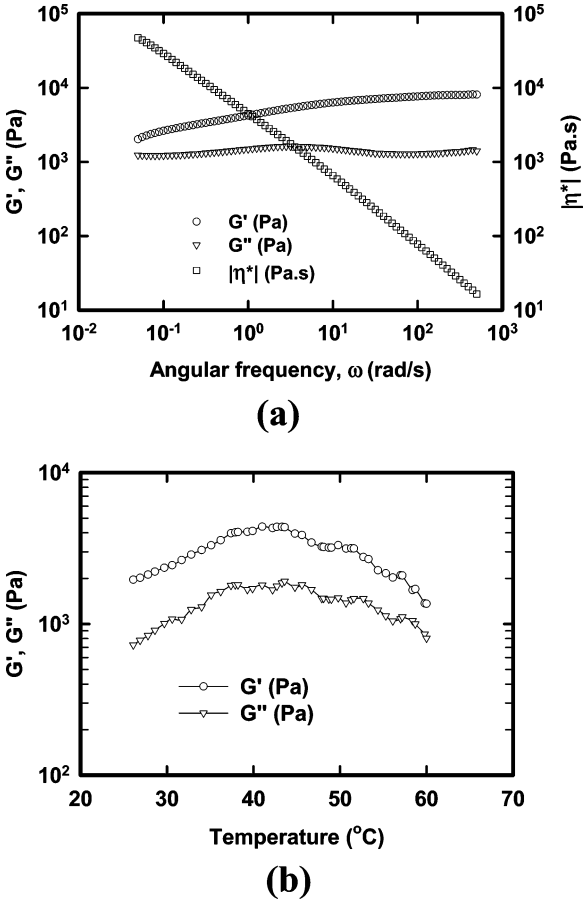

Figure 2. (a) Storage and loss moduli G' and G'' versus angular frequency, ω at $T = 25$ °C for a dynamic oscillatory flow with strain = 0.5%, demonstrating the viscoelastic response over a frequency range 0.05−500 rad/s. η^* is the complex viscosity. (b) Storage and loss moduli G' and G'' versus temperature at angular frequency ω =1 rad/s for a dynamic oscillatory flow (strain = 0.5%) demonstrating the viscoelastic response over a temperature range 25−60 °C.

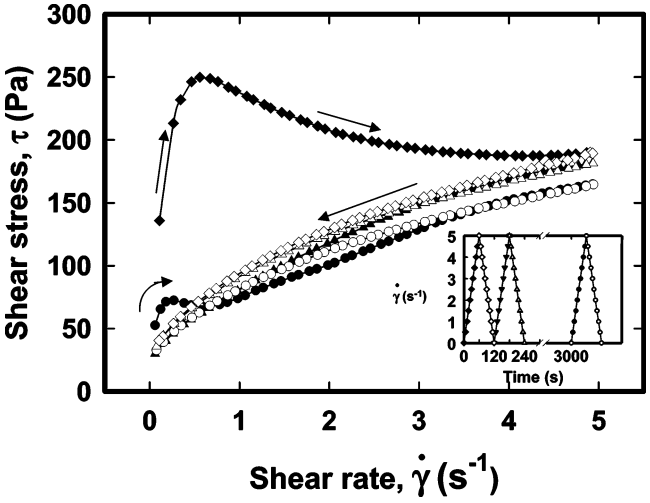

Figure 3. Shear stress behavior for the shear rate cycles shown in the inset. The first cycle shows hysteresis in the shear stress behavior. Alignment removes hysteresis by the second cycle. The lack of hysteresis in the third cycle indicates that alignment is retained after the 45min rest period.

the shear rate was linearly ramped from 0 to 5 s^{-1} over 60 s, and then back to 0 s^{-1} over the same time span (inset, Figure 3). Two cycles were performed consecutively. This was then followed by a third cycle after a 45-min rest

(53) Montalvo, G.; Valiente, M.; Rodenas, E. *Langmuir* **1996**, *12* (21), 5202.
(54) Ryu, C. Y.; Vigild, M. E.; Lodge, T. P. *Phys. Rev. Lett.* **1998**, *81* (24), 5354.
(55) Ramos, L. *Phys. Rev. Lett.* **2001**, *64*, 061502.
(56) Soltero, J. F. A.; Robles-Vasquez, O.; Puig, J. E. *J. Rheol.* **1995**, *39* (1), 235.

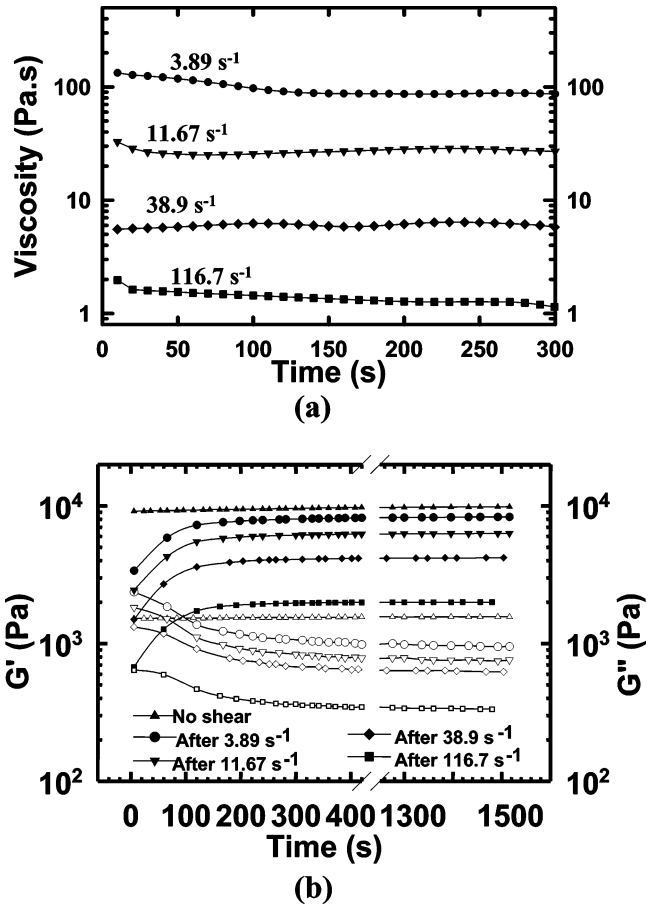

Figure 4. (a) Viscosity as a function of time when the shear rate sequence in Figure 4a is applied in steps at $T = 25$ °C. (b) Dynamic response (G', G'') of the surfactant mesophase as a function of time (for strain = 0.5% and $\omega = 1$ rad/s at $T = 25$ °C), immediately after cessation of flow at the shear rates of 0 s^{-1} (no shear), 3.89 s^{-1}, 11.67 s^{-1}, 38.9 s^{-1}, and 116.7 s^{-1}.

period. The hysteresis in shear stress in the first cycle indicates substantial microstructural changes. The second loop shows negligible hysteresis and an antithixotropic behavior. Soltero and co-workers obtained similar results with a 50% AOT solution in water.[56] These authors demonstrated that while the first hysteresis loop displayed thixotropic behavior, the consecutive loops displayed rheopectic (antithixotropic) behavior. A similar explanation can be proposed for the hysteresis observed in our system. A rate-dependent shear alignment of randomly oriented columnar hexagonal domains occurs in the first loop, along with an increase in the interdomain defects that are irreversible on the molecular time scales. In the second hysteresis cycle, the peak shear rate is the same as in the first loop (inset, Figure 3) and no thixotropy is seen, although the strain is always increasing. Once aligned, the system does not exhibit any thixotropy when sheared to the same maximum rate. Instead, a rheopectic response due to relaxations at the molecular/micellar time scales is exhibited.[56] The third loop shows a slight reappearance of hysteresis, suggesting annealing of the defects caused in the first two loops and negligible relaxation of the aligned domains or over the 45 min interval.

Separate rheological experiments in the cone and plate geometry reveal that the apparent viscosity reaches a steady value within a few seconds of the application of shear (Figure 4a). Figure 4b illustrates the dynamic viscoelastic (G', G'') response of the system immediately after the cessation of the flow. The storage moduli (G') build up as the shear is removed and reach a steady-state value in approximately 200 s, which is always lower than the steady-state G' value achieved after shearing at a lower shear rate (Figure 4b). The loss moduli (G'') on the other hand, decrease and achieve a steady-state value in the same time frame that is again lower than the G'' value achieved after shearing at a lower shear rate. The data indicate that the system regains solid response ($G' > G''$) soon after the cessation of shear. Hamley and co-workers observed a similar dynamic response while studying shear-induced orientational ordering in diblock copolymer gels.[57] These authors observed a rapid decrease in the dynamic shear moduli upon application of the deformation field (large amplitude oscillatory flow) and complete recovery upon cessation of the shear. The authors suggest that the rapid decrease in dynamic moduli is caused by a rapid increase in the density of defects in the polycrystalline gel system that anneal rapidly after shear is removed. In the AOT + lecithin system studied here, while annealing of defects may be responsible for a partial recovery of the dynamic moduli, their lower steady-state values indicate an increased order and/or domain size in the crystalline surfactant mesophase after application of shear.[58,59] Thus, application of shear does not destroy the three-dimensional structure completely but may introduce some reversible defects in the polycrystalline gel sample along with an irreversible (in the time scale of the rheological experiments of approximately 25 min) alignment of domains. This observation is revisited in the discussion of the SANS data.

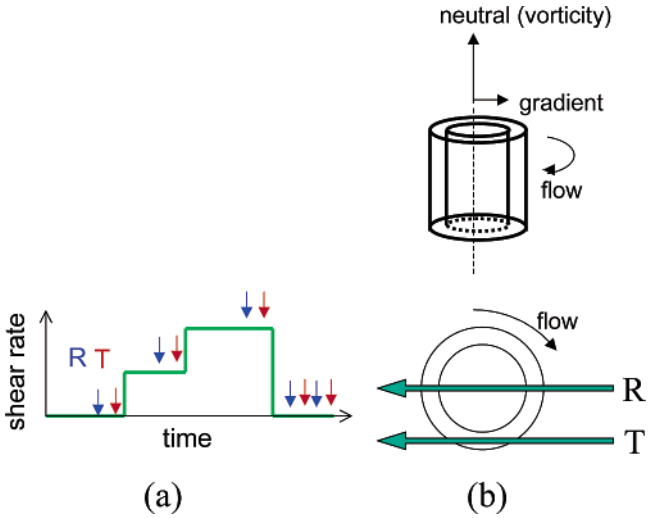

Figure 5. (a) Schematic of the shear rate sequence in the shear-SANS experiment. (b) Schematic of the Couette cell used in the shear-SANS experiment: R and T correspond to the radial and the tangential directions of the beam, respectively. Flow, gradient, and vorticity directions are shown for reference.

Characterizations by Small-Angle Neutron Scattering under Shear (Shear SANS). SANS experiments were performed to better understand microstructure alignment and subsequent relaxation. The data were collected while the system was sheared at various incremental shear rates followed by a relaxation step (Figure 5a). Data in radial and tangential modes were collected as the system was sheared at 0 s^{-1} (no shear), 3.89 s^{-1}, 11.67 s^{-1}, 38.9 s^{-1}, and 116.7 s^{-1}. The flow, flow

(57) Pople, J. A.; Hamley, I. W.; Terrill, N. J.; Fairclough, J. P. A.; Ryan, A. J.; Yu, G.-E.; Booth, C. *Polymer* **1998**, *39* (20), 4891.
(58) Chen, Z.-R.; Kornfield, J. A.; Smith, S. D.; Grothaus, J. T.; Satkowski, M. M. *Science* **1997**, *277* (5330), 1248.
(59) Makinen, R.; Ruokolainen, J.; Ikkala, O.; Moel, K. de; Brinke, G. ten; Odorico, W. De; Stamm, M. *Macromolecules* **2000**, *33*, 3441.

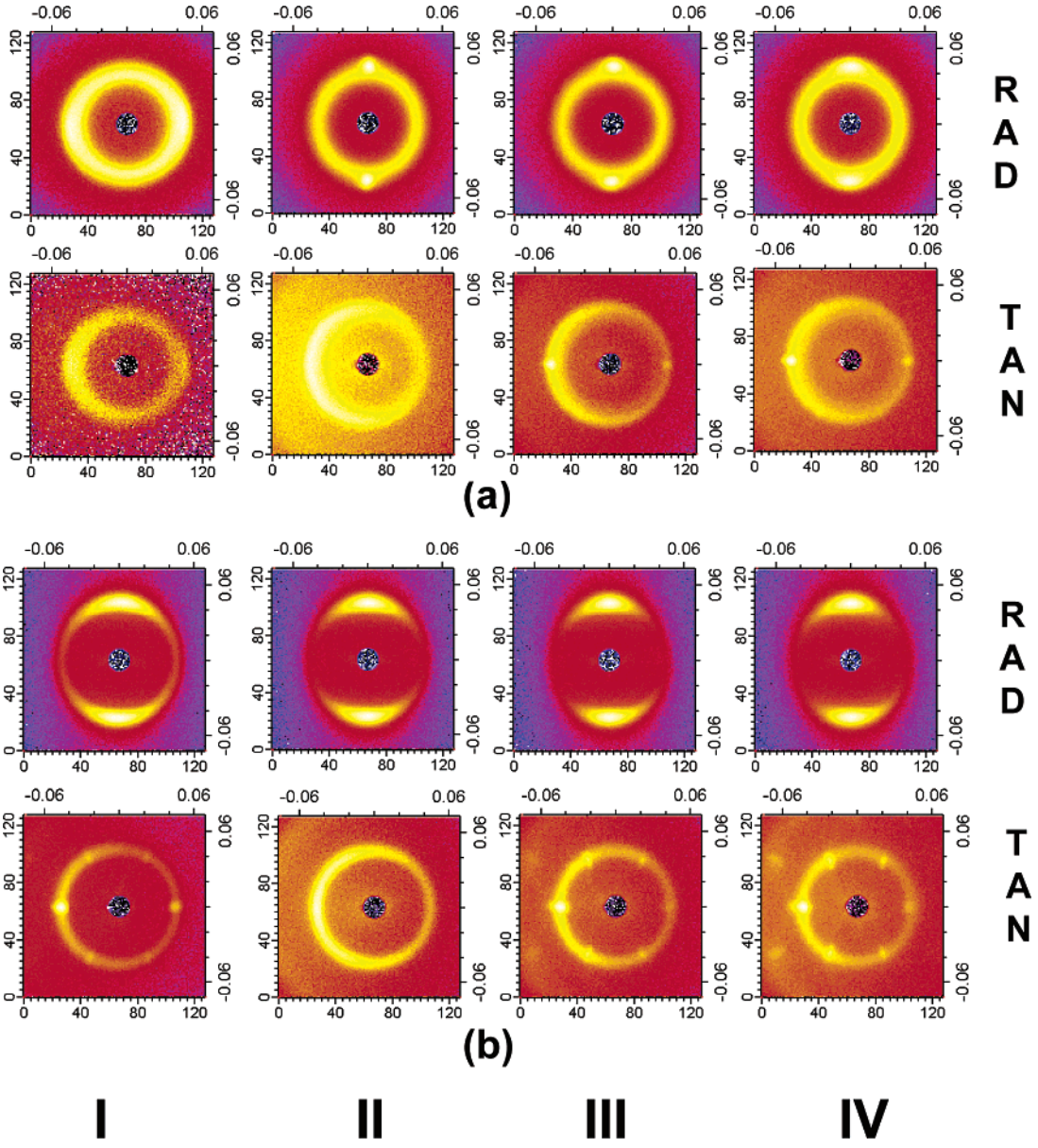

Figure 6. (a) 2D SANS profile in radial (RAD) and tangential (TAN) directions of the beam for shear experiments at 25 °C. (b) 2D SANS profile in radial (RAD) and tangential (TAN) directions of the beam for shear experiments at 41 °C. Key: I, zero shear; II, while shearing at 116.7 s^{-1}; III, immediately after shearing at 116.7 s^{-1}; III, 45 min after cessation of applied shear.

gradient, and vorticity directions are defined in Figure 5b. Data collection was initiated 40 s after each increment in shear rate. The scattering data in the radial direction examines the vorticity−flow plane, while the tangential scattering data allows observation of the vorticity−flow gradient plane. A statistically significant amount of data in the radial direction was obtained in 100 s, while each tangential direction experiment took 300 s to obtain statistically valid data.

Figure 6 shows the 2D radial and tangential scattering profiles at 25 °C and at 41 °C. The experiment at 41 °C was initiated immediately after the one at 25 °C was completed. Column I represents the scattering profile prior to application of shear. Column II represents the scattering profile during the application of shear at the highest shear rate of 116.7 s^{-1}, and in this figure we have disregarded data from lower shear rates. Column III represents the profile at rest, immediately after the maximum applied shear of 167 s^{-1}, and column IV corresponds to the scattering profile after cessation of shear for 45 min. Figure 6a-I shows that the 2D SANS intensity profile at zero shear and 25 °C is almost symmetrical both in radial and in tangential directions (a slight asymmetry is ascribed to the preshear involved in the sample loading). Clearly, asymmetrical patterns can be seen in the radial direction while the system is being sheared, although the asymmetry is not evident in the tangential direction (Figure 6a-II). Immediately after the cessation of shear (Figure 6a-III), asymmetry is also observed in the tangential direction. The asymmetry is still present 45 min after the cessation of flow (Figure 6a-IV). At 25 °C, the hexagonally arranged cylinders of the gel phase align weakly in the direction of flow. The 6-fold symmetry expected from a hexagonal arrangement is faintly visible in the tangential profile after cessation of shear. The absence of clear evidence of the 6-fold symmetry in the tangential direction of the beam during the shear alignment of hexagonal phases (as in Figure 6a-III and Figure 6b-III) has also been observed by other researchers.[60,41] The authors

(60) Pople, J. A.; Hamley, I. W.; Fairclough, J. P. A.; Ryan, A. J.; Booth, C. *Macromolecules* **1998**, *31*, 2952.

suggest that the rotational component of the flow field disturbs the single crystal structure and causes the disappearance of the hexagonal symmetry in tangential direction while the 2-fold symmetry in the radial direction is maintained. Evidently, this 6-fold symmetry in the tangential direction can be observed immediately after the cessation of the flow (Figures 6a-IV and Figure 6b-IV). Ramos and co-workers[15] and recently, Ahir and co-workers[45] have reported shear melting of the long-range two-dimensional order of the cylinders in hexagonal surfactant mesophases. In our system, while shear does seem to increase the defect density in the polycrystalline gel system (Figure 5b), it does not cause melting of the two-dimensional order of the cylinders. The typical features of shear melting are the broadening of the primary peak, a strong low-angle scattering, and the loss of higher order peaks, resulting from the "molten" (liquidlike) phases. The primary peak is not diffused in Figure 6a-III and Figure 6b-III, and low-angle scattering does not increase upon shear. We will revisit this point in the discussion of Figure 10b, where we show a quantitative comparison of the peak intensities.

When the sample sheared and relaxed at ambient temperature is heated to 41 °C (Figure 6b-I), the evidence of alignment becomes clearer both in the radial and in the tangential directions. Thus, the alignment is retained after heating the partially aligned sample at 25−41 °C. After this sample was sheared at various incremental shear rates, the scattering pattern characteristic of aligned hexagonal domains becomes more obvious (Figure 6b-III). The system retains alignment over the 45-min time interval between the data taken for Figure 6b-III and Figure 6b-IV. Scattering from both the [10] and the higher order [11] planes is clearly visible in Figure 6b-III and Figure 6b-IV.

The scattering data are further analyzed by examining the intensity as a function of azimuthal angle φ. Figure 7 shows the data during shear and after cessation of shear. Weak alignment induced from the preshear involved in the sample loading process (zero shear, Figure 7a) is noted. Alignment in the direction of flow can be seen as soon as the system is sheared (Figure 7a, rate = 3.89 s^{-1}). A comparison of peak intensities in Figure 7b with Figure 7a indicates improved alignment of hexagonal domains. Finally, the sharp peak intensities after cessation of shear for time periods up to 45 min indicate the retention of alignment. The observation clearly indicates that the relaxation times involved in the relaxation from a state of aligned domains (metastable) to one with randomly oriented domains (initial or equilibrium) are extremely large. The orientation order can be quantified in terms of the second rank order parameter (OP) by the method described by Deutsch.[61] This order parameter can be obtained from an analysis of the anisotropic structure factor peak according to

$$P_2 = 1 - \frac{3}{2N}\int_0^{\pi/2} \mathrm{d}\varphi\, I(\varphi + \pi/2)\left[\sin^2\varphi + \cos^2\varphi \sin\varphi \ln\left\{\frac{1+\sin\varphi}{\cos\varphi}\right\}\right]$$

where N is the normalization constant

$$N = \int_0^{\pi/2} \mathrm{d}\varphi\, I(\varphi + \pi/2)$$

and I is the intensity at φ, the azimuthal angle. The second rank order parameter P_2, calculated from the 2D scattering pattern in the radial direction is about 0.04 immediately after sample loading (Figure 7a, zero shear). Immediately after the application of the maximum shear rate of 116.7 s^{-1} (at ambient temperature), P_2 is 0.15. P_2 becomes 0.43 as soon as the temperature of the system is raised to 41 °C (Figure 7b, zero shear). This increase in the ordering of the system upon increasing the temperature to 41 °C coincides with the observed maxima in the dynamic moduli (Figure 2b). The value of P_2 reaches a maximum of 0.56 immediately after shearing the system at 116.7 s^{-1} at 41 °C. In a time-resolved SANS study of the structural relaxation from a shear-aligned wormlike reverse micelles formed by lecithin, Angelico and co-workers report a P_2^{max} of 0.57 at a shear rate of 10 s^{-1} that relaxes to $P_2 \sim 0$ in about 100 s. In our system P_2 does not change appreciably long after the cessation of the flow.

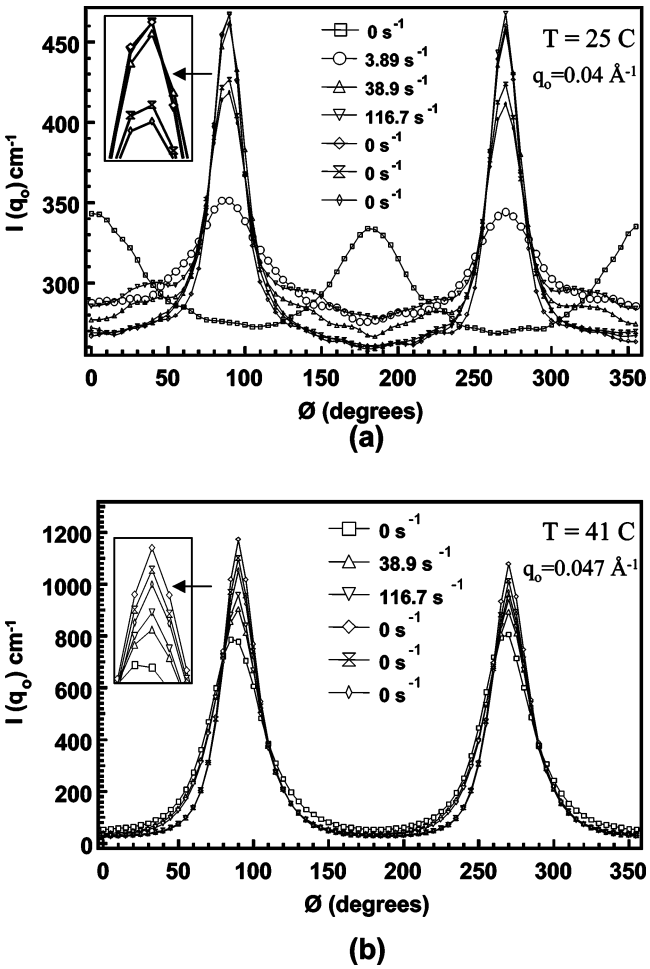

Figure 7. (a) Azimuthal variation of intensity at the primary peak position (q_o = 0.04 Å^{-1}) in the radial beam direction for different shear rates at T = 25 °C. The last three scattering curves at zero shear rates correspond to data collected after cessation of 116 s^{-1} shear, at t = 5, 15, and 45 min, respectively. (b) Azimuthal variation of intensity at the primary peak position (q_o = 0.047 Å^{-1}) in the radial beam direction for different shear rates at T = 41 °C. The last three scattering curves at zero shear rates correspond to data collected after cessation of 116 s^{-1} shear, at t = 5, 15, and 45 min, respectively.

Surfactant systems and polymer solutions at low concentrations exhibit a viscoelastic response, and in most cases a direct relationship can be established between the microstructural relaxation and stress relaxation using a single characteristic relaxation time.[62] The small-angle

(61) Deutsch, M. *Phys. Rev. A* **1991**, *44* (12), 8264.

(62) Turner, M. S.; Cates, M. E. *Langmuir* **1991**, *7*, 1590.

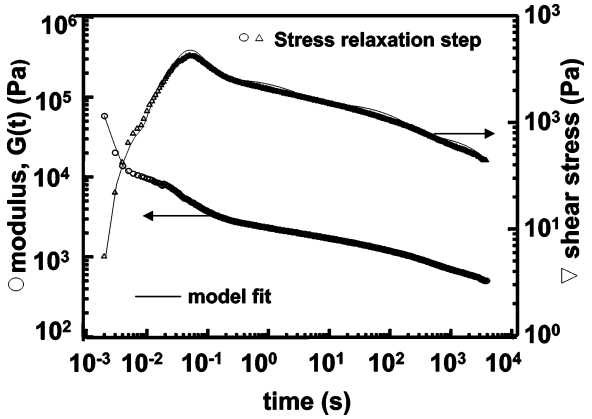

Figure 8. Stress relaxation data for 10% strain in 0.01 s (peak rate ~ 10 s^{-1}) at $T = 25$ °C; the solid line is the result of fitting the data by generalized Maxwell model discussed in the text.

oscillatory experiments indicate that this system might not have a single characteristic relaxation time. The system relaxation is characterized through the stress relaxation experiment of Figure 8. Here, a large strain (10%) is applied over 10 ms (this corresponds to a shear rate of 10 s^{-1}), and the resulting stress is monitored as a function of time. The system has a highly viscoelastic response and has a very slow stress relaxation (Figure 8). This can be understood as arising from a generalized Maxwell system with multiple relaxation times, each corresponding to a given Maxwell element.[51,17] For a system with "N" relaxation times, the extra stress tensor, τ, is given by summation of stresses in the individual elements, i.e.

$$\tau = \sum_{k=1}^{k=N} \tau_k$$

The relaxation modulus $G(t)$ is given by[51] $G(t) = \tau/\gamma_o$, where γ_o is the maximum strain (γ_o is 0.1 in our experiment). It can be shown that[51]

$$G(t) = \sum_{k=1}^{k=N} G_k e^{-t/\lambda_k}$$

where G_k and λ_k are the relaxation moduli and the relaxation times of the "kth" Maxwell element, respectively. The stress−relaxation data have been fitted using the above model. The fit obtained (solid line) involves six relaxation times (ranging from ~10^{-4} to 10^3 s) or Maxwell elements. Fits with fewer parameters (G_k and λ_k) are poor, indicating the structural complexity of the system.[63] Systems, where the complexity of the stress response necessitates the use of multiple relaxation times, have been studied.[64] Oda and co-workers have studied the shear effects in dilute aqueous solutions of a dimeric surfactant and a very similar relaxation phenomenon after cessation of the flow.[64] The authors demonstrate that the relaxation phenomena can be explained roughly by looking at the order of magnitude of the relaxation times. The authors point to three different relaxation time scales: a rapid relaxation arising from recombination of wormlike micelles, relaxation time ~10^2 s arising from diffusive rotation and randomization of anisotropic aggregates, and

(63) Xu, Y. Z.; Fong, C. F. Chan Man; De Kee, D. *J. Appl. Polym. Sci.* **1996**, *59*(7), 1099.
(64) Oda, R.; Weber, V.; Lindner, P.; Pine, D. J.; Mendes, E.; Schosseler, F. *Langmuir* **2000**, *16*, 4859.

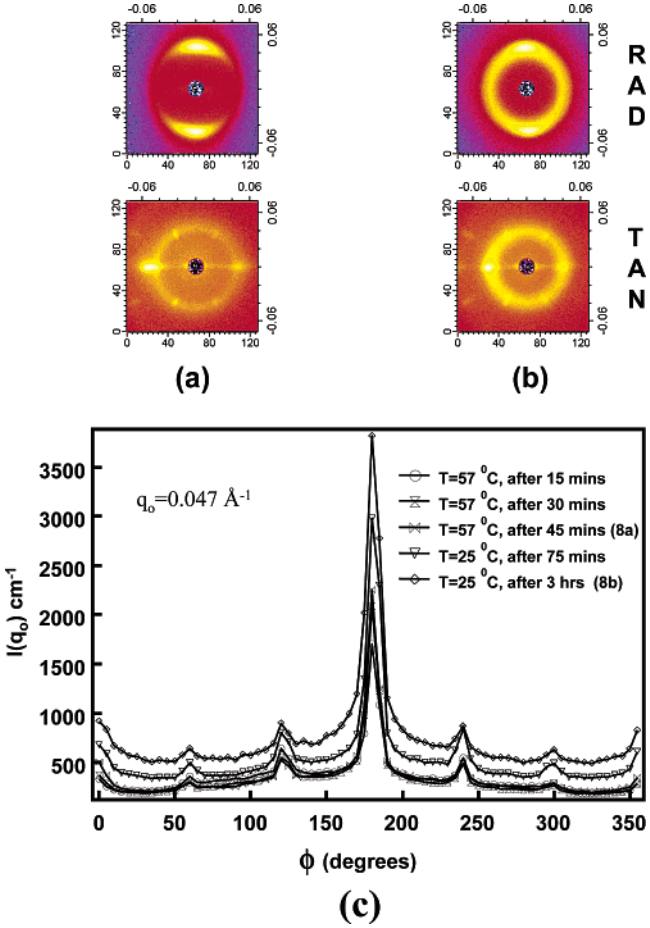

Figure 9. (a) 2D SANS profile in radial (RAD) and tangential (TAN) directions of the beam for shear experiments at 57 °C, 45 min after cessation of flow (shear rate = 0 s^{-1}). (b) 2D SANS profile in radial (RAD) and tangential (TAN) directions of the beam for shear experiments after cooling the system to 25 °C for 2 h (shear rate = 0 s^{-1}). (c) Azimuthal variation of intensity for data obtained in the tangential beam direction after the cessation of flow at $T = 57$ °C and after cooling to 25 °C (shear rate = 0 s^{-1}).

a long-time relaxation resulting from dissolution of anisotropy in these aggregates to original unsheared levels. In our system, the relaxation times on the order of 10^{-4} s may correspond to the fast molecular relaxations, and relaxation times around 10^0−10^2 s may correspond to both local recombination of cylinders (fast) and annealing of grain defects caused by shear (slow). Relaxation times on the order of 10^3 may correspond to relaxation of aligned domains. The inability to obtain in situ rheological data during shear SANS experiments limits the understanding of the correlation between stress relaxation and the relaxation of the shear-aligned domains of the gel system. Nevertheless, from the independent experiments, it is clear that both stress and the domain alignment relax very slowly.

Figure 9a illustrates the 2D SANS data 45 min after cessation of flow at 57 °C. The 2D profile indicates that shear alignment persists after heating the sample to 57 °C for extended periods. The alignment is retained when the gel phase is cooled back to 25 °C and orientation effects can be observed even after 2 h (Figure 9b). Figure 9c provides the quantitative evidence in support of this fact. At this point, the sample has undergone several steps of shear rate application and temperatures (once loaded, the sample was in the shear-SANS Couette cell for approximately 10 h), but scattering patterns indicative of

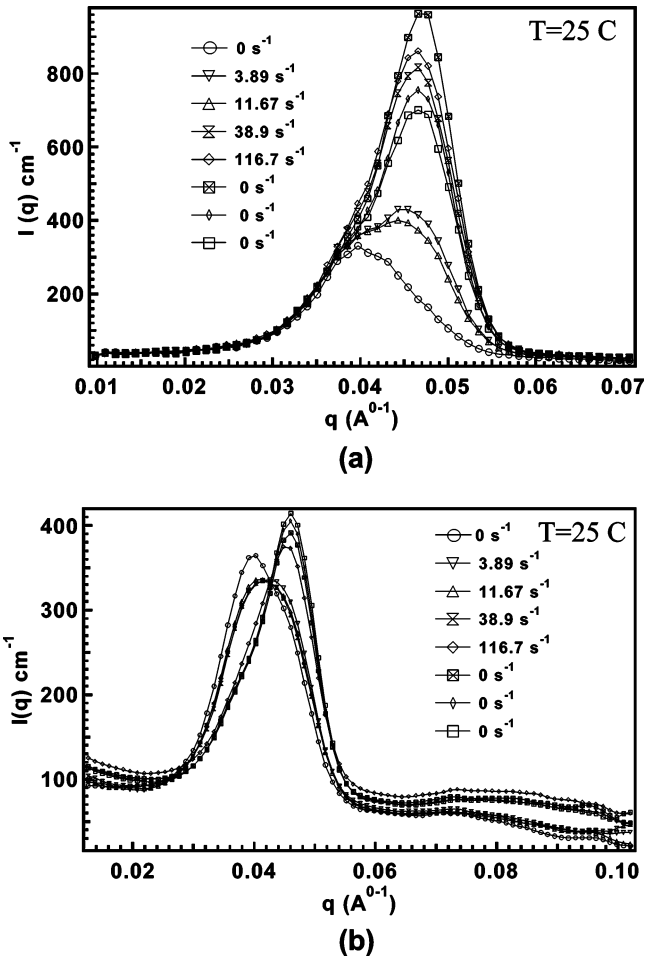

Figure 10. (a) Sector averaged ($\phi = 90°$, $\Delta\phi = 5°$) SANS data in the radial direction of the beam, for different shear rates at $T = 25$ °C. The peaks shift as the shear rate is increased. (b). Circularly averaged SANS data in tangential direction of the beam for different shear rate at $T = 25$ °C. Peak width is decreased as the shear rate is increased. (Shear rate steps are 0 s^{-1} (no shear), 3.89 s^{-1}, 11.67 s^{-1}, 38.9 s^{-1}, and 116.7 s^{-1}, followed by three relaxation steps with zero shear 0 s^{-1})

an aligned columnar hexagonal phase are still present. This observation indicates that the alignment is retained at higher temperatures once the domains are shear aligned. Thus, syntheses processes with rates strongly dependent on temperature (e.g., thermal free-radical polymerizations and ceramic syntheses) may be carried out in such prealigned systems without disrupting the alignment in the system.

Figure 10a illustrates the sector-averaged SANS data in the radial direction. As soon as shear is applied, there is a peak shift to a higher q value. We attribute this simply to enhanced mixing upon shear application. When the rigid mesophase is initially prepared by mixing its constituents, incomplete mixing may result in pockets of inhomogeneity. These pockets might contain a relatively higher concentration of surfactants in an isotropic phase, leaving the homogeneous phase with cylinders that have higher apparent water content (W_0) than a completely homogeneous gel phase ($W_0 = 70$, in this case). The pockets are annealed upon the application of shear or with an increase in temperature, and a homogeneous H_{II} phase emerges that has smaller intercylinder spacing. With higher shear rates, the primary peaks (from the sector average in the direction of flow) in the radial direction become intense and shift in the direction of higher "q". In addition to corroborating this fact, the circularly averaged

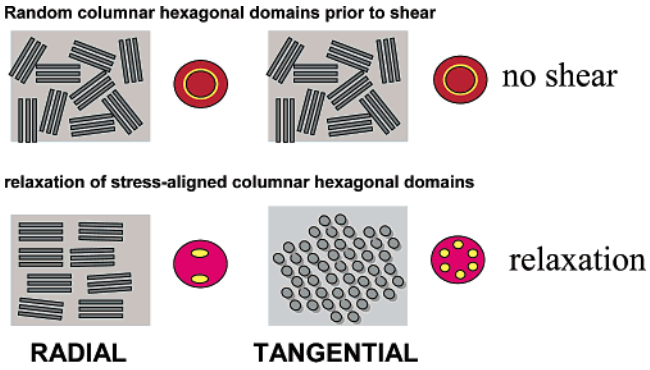

Figure 11. Proposed modes of alignment and relaxation of the columnar hexagonal mesophase.

scattering intensity profiles in the tangential direction (Figure 10b) suggest that the average domain size of the polycrystalline gel phase also increases, as indicated by sharpening of the peaks upon and after shear.[65] This explanation is supported by the SANS data, the primary peak position changes from 0.041 to 0.047 $Å^{-1}$ when the temperature is raised from 25 to 41 °C along with an increase in the scattered intensity (q_o values in Figure 7). This is also reflected in our previous work[46] where a shoulder before the primary peak is seen for $W_0 = 70$ sample at 25 °C that vanishes as the temperature is raised to 38 °C.

Figure 11 summarizes the process of shear alignment and subsequent relaxation in the gel mesophase and summarizes the results. The columnar hexagonal mesophase aligns under shear, and effective domain sizes increase. The cylinders stay aligned after cessation of shear for extended time periods, with a small relaxation of the cylinders.

Conclusions

The shear-response of a dual surfactant based gel mesophase has been investigated. Rheological characterizations indicate that the mesophase is very rigid and stable over a wide range of temperatures. The steady stress and hysteresis tests suggest that the gel domains tend to align when an external shear is applied beyond the yield stress value, and subsequent relaxation is extremely slow. Shear SANS experiments confirm these deductions. The gel domains tend to align in the direction of flow. This alignment is more pronounced when the temperature of the system is increased, and scattering patterns in the radial and tangential modes are characteristic of aligned hexagonal domains. The surfactant mesophase shows extremely slow relaxation, which is in agreement with the stress relaxation of the system, although a direct correlation has not been made due to lack of rheological data during the shear SANS experiments.

The knowledge of surfactant phase microstructure and its response to an external shear could have many applications in materials synthesis. The surfactant mesophase described here falls into the category of systems where aqueous phase synthesis may be combined with organic phase synthesis to create functional nanocomposites. The stability of the microstructure over a fairly large range of temperatures and retention of the shear-induced alignment may also be of benefit in adapting materials synthesis routes where synthesis time scales are vastly smaller than the relaxation time scales. In other words, the synthesis

(65) According to Scherrer's equation, average domain size, d_{domain}, is inversely related to the experimentally observed full width at half-maximum (fwhm) for the primary peak.

of aligned materials need not be done under shear but can be done following a preshearing excursion. Our results on the synthesis of ceramics and polymers following such observations will be presented in subsequent work.[66] Materials synthesis in these crystalline gel-like systems under shear to produce highly aligned nanomaterials and nanocomposites has significant potential.

Acknowledgment. We are grateful to Dr. Boualem Hammouda (NIST) and Dr. Lionel Porcar (NIST) for insightful discussions. Dr. Hammouda is also acknowledged for help in acquiring the SANS data. The National Institute of Standards and Technology, U.S. Department of Commerce, is gratefully acknowledged for providing the neutron research facilities used in this work through Grant NSF/DMR-9986442. The work was supported by grants from the National Science Foundation (Grants 9909912 and 0092001) and NASA (NAG-1-02070). Disclaimer: NIST does not endorse equipment or chemicals mentioned in this paper.

LA049700Y

(66) Liu, L.; Singh, M.; Agarwal, V.; John, V.; Bose, A.; McPherson, G. *J. Am. Chem. Soc.* **2004**, *126*, 2276.